Chinese Chemical Letters 31 (2020) 1322–1326

Contents lists available at ScienceDirect

Chinese Chemical Letters

journal homepage: www.elsevier.com/locate/cclet

Communication

Preparation of alumina-carbon composites with phloroglucinol-formaldehyde resin and their application in asymmetric hydrogenation

Wenrui Cai, Renjie Xiong, Cong Mao, Meitian Xiao, Yongjun Liu, Ranjith Kumar Kankala, Xueqin Zhang*

College of Chemical Engineering, Huaqiao University, Xiamen 361021, China

ARTICLE INFO

Article history:
Received 20 June 2019
Received in revised form 15 August 2019
Accepted 16 September 2019
Available online 18 September 2019

Keywords:
Phloroglucinol-formaldehyde resin
Alumina-carbon composite
Asymmetric hydrogenation
Pt nanoparticles

ABSTRACT

To overcome the shortcomings of single component carrier supported platinum (Pt)-based catalysts, herein, we demonstrate the fabrication of alumina combined mesoporous carbon to prepare a series of alumina-carbon composites and their corresponding Pt-based catalysts. The alumina-carbon composites Al@PhFC are synthesized by using phloroglucinol-formaldehyde resin as carbon source and aluminum acetylacetone as the aluminum source. Further, the effect of alumina content on the properties of the composites is investigated. The composites and catalysts are characterized by using XRD, XPS, N_2 sorption, and TEM. The Pt/Al@PhFC-1.8 composite with appropriate amounts of alumina, pore diameter, and moderate Pt nanoparticle size, resulted in 99.5% of conversion efficiency and 77.4% of optical selectivity in the asymmetric hydrogenation of ethyl 2-oxo-4-phenylbutanoate (EOPB). Interestingly, this composite can be used more than 20 times without a significant decrease in its performance.

Since Orito [1] demonstrated for the first time that Pt/γ-Al_2O_3 catalyst modified by the cinchona alkaloid could obtain excellent optical selectivity in the asymmetric catalytic hydrogenation of α-ketoesters, Pt nanoparticles have garnered enormous attention from the researches in catalysis application [2–4]. Compared to Pt/γ-Al_2O_3, whose catalytic performance explicitly declines after reusing 6 times [5], however, the mesoporous carbon-supported platinum catalysts have shown moderate selectivity but outstanding reusability owing to the high stability of support in the acidic environment [6]. For instance, Pt/FDU-15 catalyst can be reused in the similar conditions provided for more than 25 times without any distinct deactivation [7].

In this framework, our group has recently fabricated alumina-supported ordered mesoporous carbon, and a series of Al_2O_3-mesoporous carbon (Al_2O_3-MC) composites by the chelating co-assembly method [8] with resol as carbon source and aluminum acetylacetonate as the aluminum source. These composites resulted in excellent performance efficiency owing to the advantages of both alumina and ordered carbon material, in terms of mechanical strength as well as appropriate acidic sites and excellent chemical stability in an acid, high specific surface area as well as controllable pore structure, respectively. Moreover, these Al_2O_3-MC composites supported Pt nanoparticle catalysts obtained excellent enantioselectivity and reusability [9]. However, there are still some issues associated with resol as a carbon source, such as pre-synthesizing of carbon precursor is relatively complicated, low activity of phenol, resulting in a slow synthetic rate. Therefore, in this work, we use a facile one-step process to synthesize alumina-carbon composites with high-activity phloroglucinol-formaldehyde (PhF) resol instead of resol as a carbon source. The corresponding supported Pt catalysts are applied in the asymmetric hydrogenation of ethyl 2-oxo-4-phenylbutanoate (EOPB).

In this paper, we conducted the experiment to prepare alumina-carbon composites and Pt/Al@PhFC catalysts by the following methods. Firstly, alumina-carbon composites (Al@PhFC) were synthesized by the chelating co-assembly method using phloroglucinol-formaldehyde resin as a carbon source. 2.5 g of F127, 10 mL of deionized water, 12.65 mL of ethanol, and 2.5 g phloroglucinol were mixed and stirred until completely dissolved. Then, 0.17 mL of HCl solution (12 mol/L), and a certain amount of $Al(NO_3)_3{\cdot}9H_2O$ as well as acetylacetone (mole ratio of 1:2) were added successively, and stirred further for 30 min. Further, 2.36 mL of formaldehyde (37 wt%) was slowly added to the above mixture solution and stirred until liquid layering. The lower phase was stirred overnight, forming a flexible but non-sticky solid, and dried

* Corresponding author.
E-mail address: xqzhang2009@hqu.edu.cn (X. Zhang).

https://doi.org/10.1016/j.cclet.2019.09.029

at 100 °C for 12 h. Finally, the product was carbonized under nitrogen flow at 700 °C for 3 h to obtain Al@PhFC-x composites (x refers to the mass of added $Al(NO_3)_3{\cdot}9H_2O$). Then, Pt/Al@PhFC catalysts were prepared through the impregnation method [5]. Briefly, the as-synthesized alumina-carbon composites Al@PhFC were impregnated with platinum precursor (H_2PtCl_6) aqueous solution at the Pt content of ≈5 wt%) and stirred for 5 h at room temperature. Then, the mixture was evaporated to remove the solvent and further dried at 100 °C overnight to obtain Pt/Al@PhFC composites. Finally, the catalysts were reduced under hydrogen flow at 600 °C before utilization.

The as-prepared samples was characterized by X-ray diffraction (XRD), X-ray photoelectron spectroscopy (XPS), N_2 adsorption and desorption and the transmission electron microscope (TEM). The catalytic performance of the designed catalysts was evaluated for asymmetric hydrogenation of EOPB. The hydrogenation reaction was carried out in an autoclave (100 mL). Pt catalysts (100 mg), cinchonidine (CD, 10 mg), EOPB (1 mL), and acetic acid (25 mL) and H_2 (5 MPa) were used for the reaction. After finishing the reaction, the products were analyzed by GC-FID (Echrom A 90, Shanghai) equipped with capillary chiral column (CP-Chirasil-DEXCB, 25 m × 0.25 mm × 0.25 μm, Agilent Technologies). The optical yield was calculated as enantiomeric excess (*ee*) value following the formula.

$$ee\% = (|[R]-[S]|)/([R]+[S]) \times 100\%$$

The reusability test of the catalyst was performed as follows. Briefly, after the hydrogenation reaction, the mixture was centrifuged to separate the catalyst, and the catalyst was washed thrice with fresh acetic acid. Further, it was used for the next asymmetric hydrogenation reaction.

We studied the crystalline nature of the samples using XRD. The X-ray diffraction patterns were obtained on an X'Pert-Pro instrument using copper Kα radiation (40 kV, 40 mA). Fig. 1 depicts the XRD patterns of the designed Al@PhFC-x and Pt/Al@PhFC-x composites. For the Al@PhFC samples (Fig. 1a), two broad diffraction peaks centered at 22.5° and 43.5°, were observed, which could be attributed to the amorphous carbon framework [10]. It was observed from the XRD patterns that there was no characteristic diffraction peak at 37° or 49°, indicating that alumina was uniformly dispersed in these composites. It could be attributed to the addition of acetylacetone in the synthetic process of alumina-carbon composite, resulting in the formation of aluminum acetylacetonate from aluminium nitrate with higher boiling point and decomposition temperature [11]. For the catalysts (Fig. 1b), it resulted in four broad diffraction peaks at around 39.8°, 46.3°, 67.4°, and 81.3°, which could be ascribed to the (1 1 1), (2 0 0), (2 2 0) and (3 1 1) basal reflections of face-centered cubic metallic Pt (JCPDS card No. 04-0802). The intensities of diffraction peaks were enhanced with increasing the addition of $Al(NO_3)_3{\cdot}9H_2O$. Moreover, the increase of alumina might result in a decrease in the pore volume of the composite material so that the platinum particles could tend to concentrate on the surface, leading to the increase of the platinum particle size.

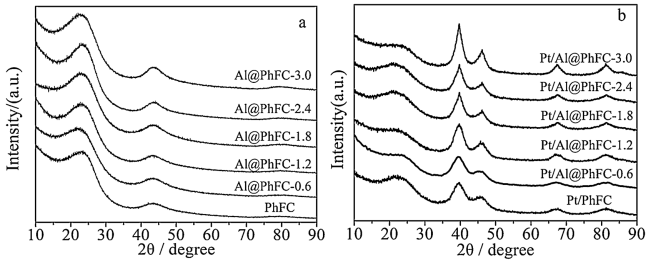

Fig. 1. XRD patterns of Al@PhFC-x composites (a) and corresponding catalysts Pt/Al@PhFC-x (b).

We further explore the elemental composition of the catalyst using XPS (Fig. 2), which was taken on a K-Alpha spectrometer with a high vacuum of 2×10^{-7} Pa. The C 1s spectra of Pt/Al@PhFC-1.8 (Fig. 2a) resulted in three types of carbon species. Three peaks were obtained by fitting and peak-splitting in the narrow spectrum of carbon, which could be attributed to -C-C-/-C = C- (284.8 eV), -C-O- (285.8 eV) and -C = O (287.1 eV), respectively [12,13], indicating that the phloroglucinol-formaldehyde resin precursor has not been completely converted to carbon. The platinum nanoparticles could form *d*-π conjugation with the benzene ring structure in the alumina-carbon composite material, which could enhance the interaction between the Pt and the composite material, and effectively reduce the Pt loss [14]. Two main peaks at 71.4 eV and 74.4 eV corresponding to Pt 4f of metallic Pt [15] and Al 2p of Al_2O_3 (Fig. 2b) [16,17], and another peak lies in 72.4 eV, demonstrated that a little amount of Pt^0 was oxidized to Pt^{2+} in process [18].

The surface area and pore textural properties measurements were recorded using N_2 adsorption-desorption isotherms at 77 K (Micrometitics ASAP 2020M + C analyzer). Table 1 displays the properties of Al@PhFC-x composites. The specific surface area increased initially and then decreased with the increase of aluminum nitrate amount. In general, the appropriate amount of alumina plays the role of supporting framework in the composite, which might result in high specific surface area. However, excess alumina could block the pores of the composite material so that the specific surface area of the composite might decrease significantly.

The N_2 adsorption-desorption isotherms and the pore size distribution curves of Al@PhFC-x composites are shown in Fig. 3. The nitrogen sorption isotherms of the samples exhibit type IV curves with H2 hysteresis loop and large uptake at low relative pressure, indicating that the composites were mainly microporous-mesoporous structures due to the removal of template and pyrolysis of phloroglucinol-formaldehyde resin at high temperature [19].

Moreover, The TEM (Tecnai G2 F20 microscope at an acceleration voltage of 100 kV) is used to characterize the catalyst supporting status. The distribution of Pt nanoparticles on the composite material can be observed in TEM images. The black dots in the figures represent the Pt particles. It was evident from the TEM images of the catalyst that the distribution of Pt nanoparticles on the composite material was very uniform with the particle size distribution ranging between 2.3–4.9 nm (Fig. 4). The corresponding mean diameter gradually increased with the increase of $Al(NO_3)_3{\cdot}9H_2O$ amount. However, the addition of excessive amounts of alumina resulted in a significant decrease in the pore volume of the composite material, tending the platinum particles to concentrate on their surface. Furthermore, the mean size of platinum particles with high dispersion in Pt/Al@PhFC-1.8 was around 3.2 nm, similar to Pt/Al_2O_3 (3.5 nm) [14], which, however much smaller than Pt/C (10.3 nm) [14]. However, it should be noted that the size of metal particles can influence the activity and selectivity and the optimum platinum particle size, which should be between 3 and 4 nm in this reaction system [20]. A feasible explanation for the poor enantioselectivity characteristic of metal particles below 2 nm is the geometric effect [21]: the small particles cannot accommodate the bulky modifier-substrate complex that occupies 20–25 surface atoms, and the non-modified reaction leads to racemic product. However, as the size of platinum nanoparticles increases, the effect of particle size can be eliminated, and the observed differences in enantioselectivity can be correlated with the surface morphology of Pt. Moreover, the control of particle size and distributions is hard due to the aggregation nature of nanoparticles. The relatively small metal

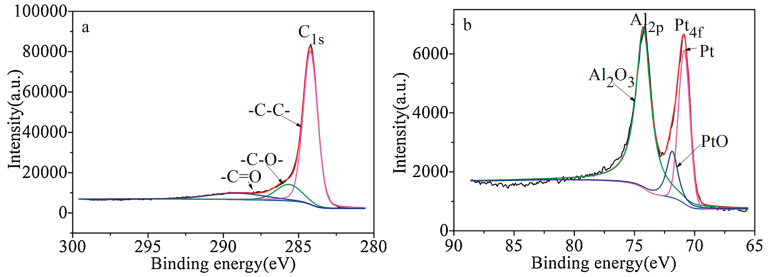

Fig. 2. XPS spectra for C_{1s} (a), Al_{2p} and Pt_{4f} (b) of Pt/Al@PhFC-1.8.

Table 1
Properties of Al@PhFC-x composites.

Entry	Sample	S_{BET} (m^2/g)	D_P (nm)	V_t (cm^3/g)
1	PhFC	430	4.5	0.69
2	Al@PhFC-0.6	477	4.9	0.53
3	Al@PhFC-1.2	447	4.1	0.46
4	Al@PhFC-1.8	416	4.2	0.39
5	Al@PhFC-2.4	374	2.6	0.27
6	Al@PhFC-3.0	315	2.7	0.21

nanoparticles (<10 nm) dispersed on the high surface area support materials, allowing excellent dispersion of Pt nanoparticles and reducing their loading amount [22]. It could probably be the reason that Pt/Al@PhFC-1.8 with the appropriate size of Pt particles yielded excellent catalytic performance.

After understanding its basic appearance and composition, we studied the catalytic performance of Pt/Al@PhFC-x in the asymmetric hydrogenation of EOPB. Table 2 shows that the catalysts maintained high conversion rates for asymmetric hydrogenation of EOPB, and corresponding optical selectivity tended to increase initially and then decreased with the increase of aluminum nitrate amount. The optical selectivity of asymmetric hydrogenation of EOPB reached a maximum of 77.4% when the amount of aluminum nitrate was around 1.8 g. In contrast, Pt/Al@PhFC-1.8 obtained the highest *ee* value and conversion efficiency of 77.4% and 99.5%, respectively, which are comparatively better than the commercially-available Pt/C, Pt/MC, Pt/MS catalysts and Pt/CMK-3. On one hand, The CD-modified Pt/Al_2O_3 catalysts induce good enantioselectivity for the asymmetric hydrogenation of α-functionalized ketones. However, the intrinsic drawback of Al_2O_3 with inferior stability in acetic acid limits the reusability of Pt/Al_2O_3 catalysts due to peptization of alumina under the acidic conditions. The activity of commercial Pt/Al_2O_3 catalyst is significantly reduced after recycling 3 times. On the other hand, commercial carbon materials have better physicochemical stability, but the Pt/C catalysts have no significant advantage of the optical selectivity for the asymmetric hydrogenation of α-functionalized ketones. Herein, Al@PhFC, as a two-component support material, combines the advantages of Al_2O_3 and carbon material. Firstly, Pt/Al@PhFC presents excellent reusability predominantly attributing to the good stability of the mesoporous carbon structure in the acidic conditions [6]. Secondly, alumina in Al@PhFC also can form electrophilic $O^+[Al(OAc)_2]_3$ under acetic acid conditions [24]. These ions can adsorb chiral modifiers and play a part in the construction of chiral environments. In addition, the introduction of alumina in the mesoporous carbon skeleton can promote the formation of $Pt^{\delta+}$ species, and the $Pt^{\delta+}$ may promote the reaction with enhanced enantioselectivity [25]. Moreover, the presence of alumina can

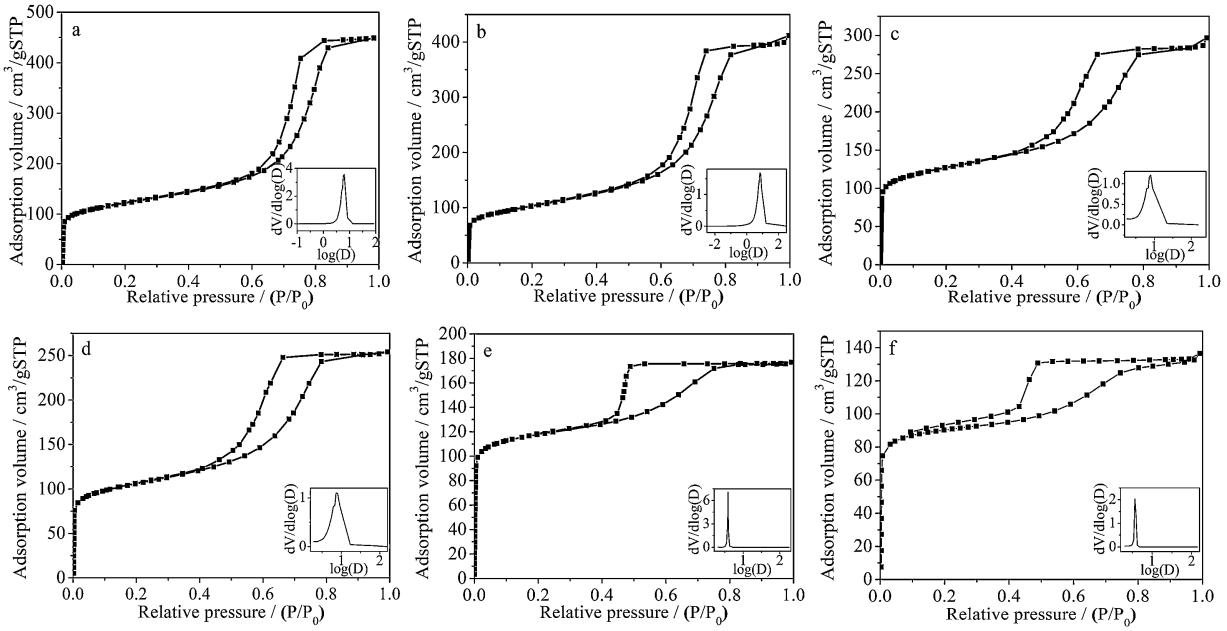

Fig. 3. Nitrogen sorption isotherms for PhFC (a), Al@PhFC-0.6 (b), Al@PhFC-1.2 (c), Al@PhFC-1.8 (d), Al@PhFC-2.4 (e) and Al@PhFC-3.0 (f). The insets are the corresponding pore size distribution curves based on the adsorption branch of isotherm.

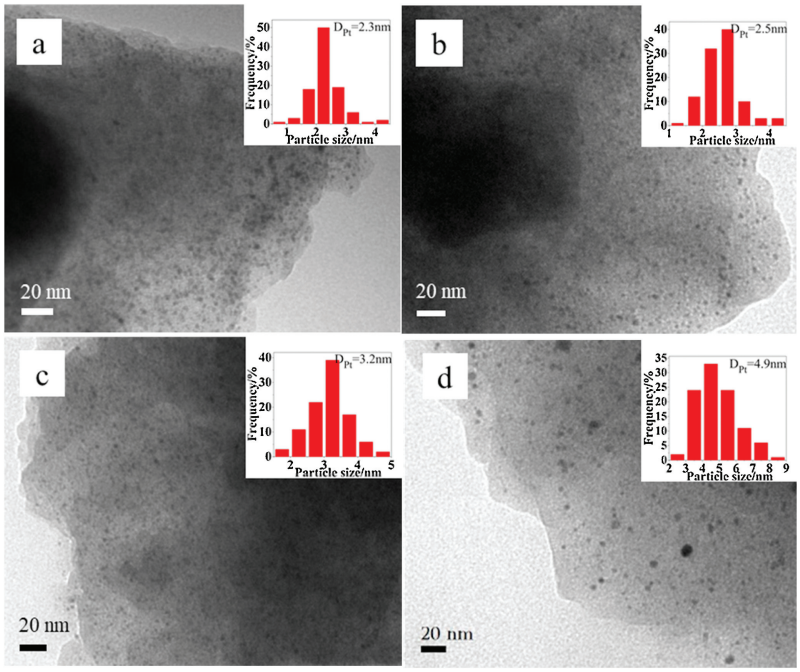

Fig. 4. TEM images of a) PhFC, b) Pt/Al@PhFC-1.2, c) Pt/Al@PhFC-1.8 and d) Pt/Al@PhFC-2.4. D_{Pt} is the mean size of platinum particles.

Table 2
The catalytic performance of Pt/Al@PhFC-x in the asymmetric hydrogenation of EOPB.

Entry	Sample	Conversion (%)	*ee* (%)
1	Pt/PhFC	99.0	70.5
2	Pt/Al@PhFC-0.6	99.1	73.3
3	Pt/Al@PhFC-1.2	98.7	75.8
4	Pt/Al@PhFC-1.8	99.5	77.4
5	Pt/Al@PhFC-2.4	99.3	74.9
6	Pt/Al@PhFC-3.0	98.9	69.3
7	Pt/Al_2O_3[a]	98.9	83.5
8	Pt/C[a]	96.9	69.2
9	Pt/MC[a]	70.7	67.5
10	Pt/MS[b]	100.0	70.8
11	Pt/CMK-3[c]	93.4	64.3

[a] The catalytic performance of commercial Pt/Al_2O_3 catalyst, commercial Pt/C catalyst and Pt/MC refers to the catalyst with Pt nanoparticles supported on mesoporous carbon from Ref. [8].
[b] Pt/MS refers to the catalyst with Pt nanoparticles supported on mesoporous silica from Ref. [23].
[c] Pt/CMK-3 refers to the catalyst with Pt nanoparticles supported on ordered mesoporous carbon from Ref. [14].

enhance the rigidity of the carbon skeleton structure and facilitate the maintenance of its mesoporous structure during the high temperature calcination and reduction processes [8]. In addition, it is conducive to the diffusion and adsorption of raw materials and chiral modifiers on the active metal surface. A certain amount of alumina could promote the asymmetric hydrogenation of EOPB, but excess alumina would lead to the blockage of pores and interfere with the diffusion of reactants [24,25].

It should be noted that the reusability of the catalyst is a fundamental attribute to be considered for catalysis application. The recycling experiments were processed by using Pt/Al@PhFC-1.8 in successive asymmetric hydrogenation reactions of EOPB. Pt/Al@PhFC-1.8 resulted in high durability and stability in the recycling process. After recycling 20 times, the optical selectivity and conversion could maintain over 77% and 90%, respectively (Fig. 5). In our previous work, Pt/15AM, using resol as a carbon source in the preparing process, could be reused more than 23 times. The reusability of Pt/Al@PhFC-1.8 could reach about 20 times, but the *ee* values were slightly lower than Pt/15AM. We found that the catalytic activity of the catalysts always decreased significantly after about 20 cycles through several reusability experiments. Compared to Pt/Al@PhFC catalyst, traditional Pt/Al_2O_3 showed much more inferior reusability, which mainly caused by the Pt leaching and the peptization of alumina in acetic acid [14,26]. The excellent reusability of Pt/Al@PhFC was mainly ascribed to the good stability of the mesoporous carbon structure in acid conditions [6]. Furthermore, Pt particles could be stability by the π-donating from the benzene rings of carbon composites to Pt particles [14]. In addition, one-step 600 °C reduction may result

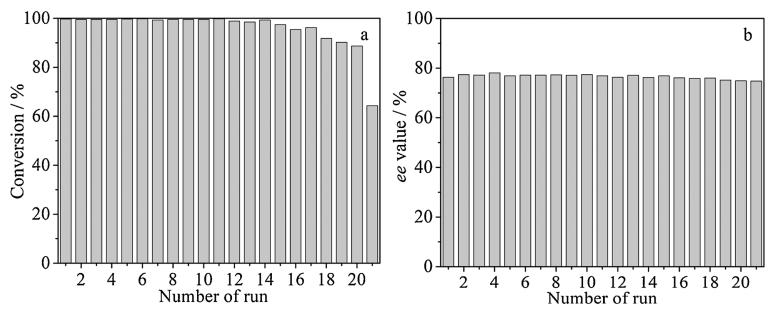

Fig. 5. Reusability of Pt/Al@PhFC-1.8 for the asymmetric hydrogenation of EOPB.

in more facet Pt particles, which had much stronger interaction with the support [27]. These three factors all reduced the Pt loss during each cycle in acetic acid resulting in their excellent reusability. Compared with our previous works, it is noteworthy that we used the one-step process to synthesize alumina-carbon composite with high-activity phloroglucinol-formaldehyde as carbon source. No need to synthesize carbon precursor in advance effectively improved the reaction rate and simplified the preparation process.

In summary, Pt/Al@PhFC-x catalysts were successfully prepared by chelating co-assembly and impregnation method. The catalysts were tested by using XRD, XPS, N_2 sorption, and TEM. The Pt/Al@PhFC-1.8 showed excellent catalytic performance with appropriate amounts of alumina, pore diameter, and moderate Pt nanoparticle size. The Pt/Al@PhFC-1.8 yielded 99.5% conversion and 77.4% optical selectivity for asymmetric hydrogenation of EOPB, which could be repeated more than 20 times without any significant loss of its efficiency. Compared with Al_2O_3-MC that made of resol as a carbon source, the one-step synthesis of Al@PhFC could improve the preparation rate and simplify the experimental steps. This work will potentially afford a new perspective for the design and synthesis of the support of Pt/cinchona catalytic system.

Acknowledgments

This work was supported by the National Natural Science Foundation of China (Nos. 51603077, 21603077), the Natural Science Foundation of Fujian Province (No. 2019J01077), Marine High-Tech Industry Development Project of Fujian Province [No. (2016)17], Promotion Program for Young and Middle-Aged Teacher in Science and Technology Research of Huaqiao University (No. ZQN-PY516) and Subsidized Project for Postgraduates' Innovative Fund in Scientific Research of Huaqiao University.

References

[1] Y. Orito, S. Imai, S. Niwa, J. Chem. Soc. Jpn. (1980) 670–672.
[2] L.L. Lou, T. Yang, W.J. Yu, et al., Catal. Today 298 (2017) 197–202.
[3] T. Yang, L.L. Lou, W.J. Yu, et al., ChemCatChem 9 (2017) 458–464.
[4] W.J. Yu, L.L. Lou, K. Yu, et al., RSC Adv. 6 (2016) 52500–52508.
[5] J.T. Wehrli, A. Baiker, D.M. Monti, et al., J. Mol. Catal. 61 (1990) 207–226.
[6] R. Xing, N. Liu, Y. Liu, et al., Adv. Funct. Mater. 17 (2007) 2455–2461.
[7] X. Li, Y. Shen, X. Rong, et al., Catal. Lett. 122 (2008) 325–329.
[8] Q. Li, X.Q. Zhang, M.T. Xiao, et al., Catal. Commun. 42 (2013) 68–72.
[9] X.Q. Zhang, Q. Li, M.T. Xiao, et al., Appl. Catal. A-Gen. 480 (2014) 50–57.
[10] H. Wang, A. Wang, X. Wang, et al., Chem. Commun. (Camb.) 22 (2008) 2565–2567.
[11] P. Rodriguez, B. Caussat, X. Iltis, et al., Chem. Eng. J. 211-212 (2012) 68–76.
[12] E. Miloskovska, C. Friedrichs, D. Hristova-Bogaerds, et al., Macromolecules 48 (2015) 1093–1103.
[13] S.D. Gardner, C.S.K. Singamsetty, G.L. Booth, et al., Carbon 33 (1995) 587–595.
[14] B. Li, X.H. Li, H.N. Wang, et al., J. Mol. Catal. A-Chem. 345 (2011) 81–89.
[15] L.H. Nie, J.G. Yu, X.Y. Li, et al., Environ. Sci. Technol. 47 (2013) 2777–2783.
[16] B.J. Tan, K.J. Klabunde, P.M.A. Sherwood, J. Am. Chem. Soc. 113 (1991) 855–861.
[17] F.A. Marchesini, S. Irusta, C. Querini, et al., Appl. Catal. A-Gen. 348 (2008) 60–70.
[18] J. Stein, L.N. Lewis, Y. Gao, et al., J. Am. Chem. Soc. 121 (1999) 3693–3703.
[19] Z. Sun, B. Sun, M. Qiao, et al., J. Am. Chem. Soc. 134 (2012) 17653–17660.
[20] D.Y. Murzin, E. Toukoniitty, React. Kinet. Catal. Lett. 90 (2007) 19–25.
[21] F. Hoxha, N.V. Vegten, A. Urakawa, et al., J. Catal. 261 (2009) 224–231.
[22] H. Du, C.X. Zhao, J. Lin, et al., Chem. Rec. 18 (2018) 1365–1372.
[23] M.U. Azmat, Y. Guo, Y. Guo, et al., J. Mol. Catal. A-Chem. 336 (2011) 42–50.
[24] M. Bartók, K. Balázsik, G. Szöllösi, et al., J. Catal. 205 (2002) 168–176.
[25] H.N. Wang, X.H. Li, Y.M. Wang, et al., ChemCatChem 2 (2010) 1303–1311.
[26] K. Balázsik, M. Bartók, J. Mol. Catal. A-Chem. 219 (2004) 383–389.
[27] J. Liu, ChemCatChem 3 (2011) 934–948.